### Title
Mapping the sensitivity of T cells with an optical trap: Polarity and minimal number of receptors for Ca2+ signaling




### Journal
Proceedings of the National Academy of Sciences of the United States of America, 96(15)

### ISSN
0027-8424



### Authors
Wei, Xunbin
Tromberg, Bruce J
Cahalan, Michael D



### Publication Date
1999-07-20

### DOI
10.1073/pnas.96.15.8471

*Proc. Natl. Acad. Sci. USA*
Vol. 96, pp. 8471–8476, July 1999
Biophysics

# Mapping the sensitivity of T cells with an optical trap: Polarity and minimal number of receptors for $Ca^{2+}$ signaling

XUNBIN WEI*†, BRUCE J. TROMBERG*†, AND MICHAEL D. CAHALAN*‡

*Department of Physiology and Biophysics, and †Laser Microbeam and Medical Program, Beckman Laser Institute, University of California, Irvine, CA 92697

*Edited by Erwin Neher, Max Planck Institute for Biophysical Chemistry, Goettingen, Germany, and approved May 24, 1999 (received for review March 8, 1999)*

**ABSTRACT** **Contact with antigen-presenting cells (APCs) initiates an activation cascade within T lymphocytes, including a rise in cytosolic calcium, lymphokine production, and cell division. Although T cell–APC physical contact is required for an immune response, little is known about the patterns of cellular interactions and their relation to activation. Calcium imaging combined with an optical trap enabled the T cell contact requirements and polarity to be investigated at the single-cell level. APCs or anti-CD3 mAb-coated beads were trapped with a laser and placed at different locations along the T cell, which has a polarized appearance defined by the shape and direction of crawling. T cells were 3-fold more sensitive to APC contact made at the leading edge of the T cell than with contact made at the tail. Anti-CD3 mAb-coated 6-$\mu$m beads induced calcium signaling with ≈10-fold higher frequency and ≈4-fold shorter latency on contact with the leading edge of the T cell than on contact with the trailing edge. Alterations in antibody density (2 to 500 per $\mu m^2$) and bead size (1 to 6 $\mu$m in diameter) were used to determine the spatial requirements and the minimal number of receptors which must be engaged to transmit a positive signal. T cell response percentage, latency, and calcium-signaling pattern (transient vs. sustained or oscillatory) depended on antibody density on the bead. The presence of ≈170 anti-CD3 mAb within the contact area elicited a detectable T cell calcium response. We propose here that engagement of no more than 340 T cell receptors (≈1% of the total on the cell) is sufficient to initiate $Ca^{2+}$ signaling. The minimal contact area was ≈3 $\mu m^2$.**

T cell activation is a complex, multistep process involving a number of molecules, including the T cell receptor (TCR) binding to its ligand, a specific peptide bound to a MHC molecule on the antigen-presenting cell (APC; ref. 1). Although direct cell–cell contact is required for T cell activation, little is known about the patterns of cellular interaction and their relation to activation. Assuming that a single-hit TCR engagement by its ligand results in internalization of the activated receptor, Viola, Lanzavecchia, and coworkers (2, 3) measured the number of surface TCRs after stimulation and found that T cells "count" the number of triggered TCRs and respond to produce IFN-$\gamma$ when a threshold of ≈8,000 TCRs is reached. Costimulatory signals lowered the activation threshold to ≈1,500 TCRs. Here, we report the development and application of an optical-trap-based single-cell assay to study the contact requirements for T cell activation and the minimum number of TCRs that must be engaged to initiate the intracellular calcium signal ($[Ca^{2+}]_i$), an event that occurs much earlier than cytokine production.

Optical traps (tweezers) use photon momentum transfer to grasp and manipulate microscopic dielectric particles, such as beads (microspheres), cellular organelles, and cells. A number of biological applications have been demonstrated with "optical tweezers" (4), including sorting and isolation of cells, organelles, and chromosomes; measuring the mechanical properties of cytoskeletal assemblies, biopolymers, and membranes; and measuring mechanical forces generated during DNA transcription (5, 6). In this work, we use optical tweezers to present microsphere-immobilized anti-CD3 mAb at varying surface densities to well defined regions of individual T cells. This general approach is ideal for investigating ligand-based cellular interactions, because the contact geometry, timing, and nature of the ligand can be specified exactly under physiological conditions. Using calcium imaging and an optical trap, we recently showed that murine hybridoma hen egg lysozyme-restricted $CD4^+$ T cells (1E5) are polarized antigen sensors (7). Here, we extend these studies to address the spatial and temporal contact requirements for T cell activation and the minimum number of receptors that must be engaged to transmit a $[Ca^{2+}]_i$ signal.

## MATERIALS AND METHODS

**Cell Culture.** The murine hen egg lysozyme-restricted, $CD4^+$ T cell (1E5; ref. 8) and MHC II-restricted B cell (2PK3) hybridomas (a gift from A. Sette, Cytel, San Diego) were grown in RPMI medium 1640 containing 10% (vol/vol) FBS, 10 mM Hepes, 10 $\mu$M $\beta$-mercaptoethanol, and 1% each of nonessential amino acids, glutamine, and sodium pyruvate. Cells were maintained in a humidified incubator at 37°C with 5% $CO_2$, 95% air. The 1E5 cells were adherent to plastic flasks at 37°C and were resuspended for collection by gentle shaking at room temperature. Antigen-presenting 2PK3 B cells were incubated with 10 $\mu$g/ml hen egg lysozyme for 3–12 h. This protocol produced a maximal response from 1E5 T cells as judged by a contact-dependent $[Ca^{2+}]_i$ response from ≈70% of cells.

**Antibody Coating on Beads.** T cells were also probed with anti-mouse CD3$\varepsilon$ mAb-coated beads. We used various sizes of polystyrene beads (1–6 $\mu$m in diameter; Interfacial Dynamics Corporation, Portland, OR) stabilized with sulfate charges. Beads were initially coated with 100 $\mu$g/ml anti-hamster Fc IgG mAb in 25% (vol/vol) PBS for 1 h at room temperature and then with varying concentrations of FITC-conjugated hamster anti-mouse CD3 mAb of known fluorescein/protein ratio for 1 h. Beads coated with anti-hamster IgG mAb alone did not activate T cells (0%; 0 of 100). The number of anti-CD3 mAb on single beads was quantified by analysis with a fluorescence-activated cell sorter (FACS) to compare FITC-conjugated mAb-coated beads with a standard curve of microbeads labeled with defined numbers of fluorescein molecules (Flow Cytometry Standards Corporation, San Juan, PR).

The publication costs of this article were defrayed in part by page charge payment. This article must therefore be hereby marked "*advertisement*" in accordance with 18 U.S.C. §1734 solely to indicate this fact.

PNAS is available online at www.pnas.org.

This paper was submitted directly (Track II) to the *Proceedings* office.

Abbreviations: APC, antigen-presenting cell; TCR, T cell receptor; FACS, fluorescence-activated cell sorter.

‡To whom reprint requests should be addressed. e-mail: mcahalan@uci.edu

The coating variation between beads was relatively small (typically 15% coefficient of variation). Under fluorescence microscopy, the beads appeared round and uniformly fluorescent. Throughout the experiment, the beads did not encounter serum proteins to prevent their adsorption and contribution to the adhesion between the bead and cell.

**Optical Trapping.** The geometry of T cell–APC or T cell–bead contact was manipulated by using a tunable, near-infrared titanium:sapphire laser producing a trapping beam at ≈820 nm (9). The trapping laser was introduced via the TV port of a Zeiss Laser Scanning Confocal microscope (LSM 410). A short-pass (720-nm) dichroic reflector was used to separate trapping and fluorescence-excitation beams. A ×100 1.3 numerical aperture Neofluor objective focused the near infrared and visible beams, resulting in 20 mW of trapping power at the focal plane. This arrangement allowed trapping and fluorescence-based $[Ca^{2+}]_i$ measurements on the same cells. A wavelength of 820 nm for the optical trap was chosen to minimize cell damage (10).

**$[Ca^{2+}]_i$ Imaging.** To measure T cell $[Ca^{2+}]_i$ on the LSM microscope, 1E5 cells were coloaded with a combination of Fura Red/acetoxymethyl (5 μM) and Oregon Green/acetoxymethyl (2 μM; Molecular Probes), two long-wavelength $Ca^{2+}$ indicators that respond to the 488-nm excitation line of the argon laser. After dye loading, the cells were washed and maintained throughout in mammalian Ringer solution containing (in mM): 160 NaCl, 4.5 KCl, 2 $CaCl_2$, 1 $MgCl_2$, 10 Hepes (pH = 7.4; osmolality 290–310 milliosmol/kg), supplemented with 11 mM glucose. Cells loaded for 1.5 h at 37°C produced a red-to-green shift when $[Ca^{2+}]_i$ was elevated. This shift was quantified by scanning cells with the argon laser and dividing the fluorescence-intensity signals from two photomultipliers with emission bands of 510–555 nm (green) and >610 nm (red). In these experiments, a single 2PK3 cell or anti-CD3 mAb-coated bead was held in the trap on a heated stage (37°C) and positioned so that it made contact with a particular region (leading edge, mid section, or trailing edge) of a dye-loaded T cell. Once the cells or beads were positioned, the trapping beam was cut off, and 488-nm laser excitation was performed. A third photomultiplier collected a $Ca^{2+}$-insensitive blue emission band (400–480 nm) from incandescent illumination, which was used to produce a bright field image. There were 100–150 scans made at 4-s intervals to determine whether a $[Ca^{2+}]_i$ increase occurred in the T cell after contact with the APC or bead. T cells not responding within 400 s were scored as unresponsive. The latency of the T cell $[Ca^{2+}]_i$ response was defined as a time delay between cell–cell/bead contact and a detectable $[Ca^{2+}]_i$ rise within the responding T cell. $[Ca^{2+}]_i$ was estimated by dividing 488-nm-excited green and red fluorescence images pixel by pixel. A positive response was confirmed by a sharp increase in estimated $[Ca^{2+}]_i$ of at least 50% over basal levels. Calibration was performed by measuring fluorescence intensities at very low and saturating $[Ca^{2+}]_i$ in cells by using 1 μM ionomycin and either 1 mM EGTA for $R_{min}$ or 10 mM $Ca^{2+}$ for $R_{max}$ (where $R$ is the ratio of 488-nm-excited green-to-red fluorescence intensity) and applying the equation of Grynkiewicz *et al.* (11).

**Contact-Area Estimation.** The flexibility of positioning with the optical tweezers allowed us to choose the same T cell–bead contact geometry, including similar polarized T cell shape and similar contact geometry with the leading edge of the T cell. The contact area was assumed to form a spherical cap with a solid angle of $2\alpha$ on the bead and estimated by the equation $C = 2\pi R^2(1 - \cos\alpha)$, where C is the contact area and $\alpha$ is half of the solid angle for the contact cap. The contact geometry usually does not change until after the $[Ca^{2+}]_i$ rise. For beads of the same size, the contact area was essentially the same for each T cell–bead pair.

## RESULTS AND DISCUSSION

**T Cell Functional Polarity Identified with an Optical Trap.** In these experiments, a single murine hybridoma MHC class II-restricted B cell (2PK3) or a polystyrene bead coated with mAbs to the TCR CD3ε subunit was held and manipulated by the trap for about 10 s so that it made contact with a particular region of a T cell, which has a polarized appearance defined by the shape and direction of crawling. The T cells were loaded with Fura Red and Oregon Green, two cytoplasmic $[Ca^{2+}]$ indicators. Before contact, $[Ca^{2+}]_i$ was uniformly low in the T cells. Once the cells or beads were positioned, the trapping beam was cut off. The subsequent $[Ca^{2+}]_i$ response was detected as an emission shift from red to green (Fig. 1).

T cells were 3-fold more sensitive and responded with shorter latencies to APC contact made at the leading edge of the T cell than with contact made at the tail (Fig. 1; Table 1). When stimulated by 6.2-μm-diameter beads coated with anti-CD3 mAb, the polarity was even more dramatic; response percentages were ≈10-fold higher with contact at the leading edge (87%). In contrast, only 4 of 55 cells responded to contact at the trailing edge. T cells contacted by either an APC or an antibody-coated bead entered a dynamic and reproducible program in the first 10–20 min, including a rise in $[Ca^{2+}]_i$, in the form of either a transient response or an oscillation, changes in shape and motility, engulfment followed by partial disengagement of the APC or bead, and stabilization of the contact.

To rule out the possibility that a simple difference in engagement area accounts for the polarized response, smaller beads (2.5 μm in diameter) were examined. With 2.5-μm beads, head and tail contact areas are approximately the same (4.9 $\mu m^2$). Despite this similarity, the polarized response persists (Table 1). This result implies that a localized molecular mechanism governs the T cell polarity to antigen.

T cell–B cell contact during antigen presentation involves a number of molecular pairs, any of which may contribute to the observed polarity, e.g., TCR/MHC:peptide, CD28/B7, or LFA-1/ICAM-1 (12). Although the TCR and other surface molecules appear uniformly distributed before activation, there may be functional differences because of aggregation ability and/or localization of transduction elements such as kinases at the leading edge (13, 14). The lack of accessory molecules on anti-CD3 mAb-coated bead is probably responsible for the observed more dramatic polarity, compared with APC stimulation.

T cell polarity after contact with an APC has been well documented on the basis of plasma membrane protein clustering (15), cytoskeletal movement (16), organellar rearrangement (17, 18), and cytokine production. In addition to reorganization triggered by cell–cell contact, T cells are motile and thus possess some intrinsic polarity even before they contact the APC. Here, we confirm that T cells are polarized antigen sensors to either APC or immobilized anti-CD3 mAb stimulation. In contrast, the APCs did not seem to have polarity when engaged with T cells, a result also observed by Wülfing *et al.* (19). The inherent T cell polarity may play an important role in ensuring the high sensitivity of T cells in crowded environments such as lymph nodes, where most antigen is detected.

**TCR Threshold for Initiating the T Cell $[Ca^{2+}]_i$ Signal.** The response of T cells to antigen depends on the number of engaged TCRs. To investigate the receptor threshold for initiating the $[Ca^{2+}]_i$ signal, we varied the anti-CD3 antibody density on 5-μm-diameter beads. The number of antibodies on single beads was quantified by using flow cytometry (Fig. 2). The anti-CD3 antibody-coated beads at densities ranging from 2 per $\mu m^2$ to 500 per $\mu m^2$ were then manipulated with an optical trap and placed at the leading edge of T cells, and the subsequent $[Ca^{2+}]_i$ response was monitored. Both the percent-

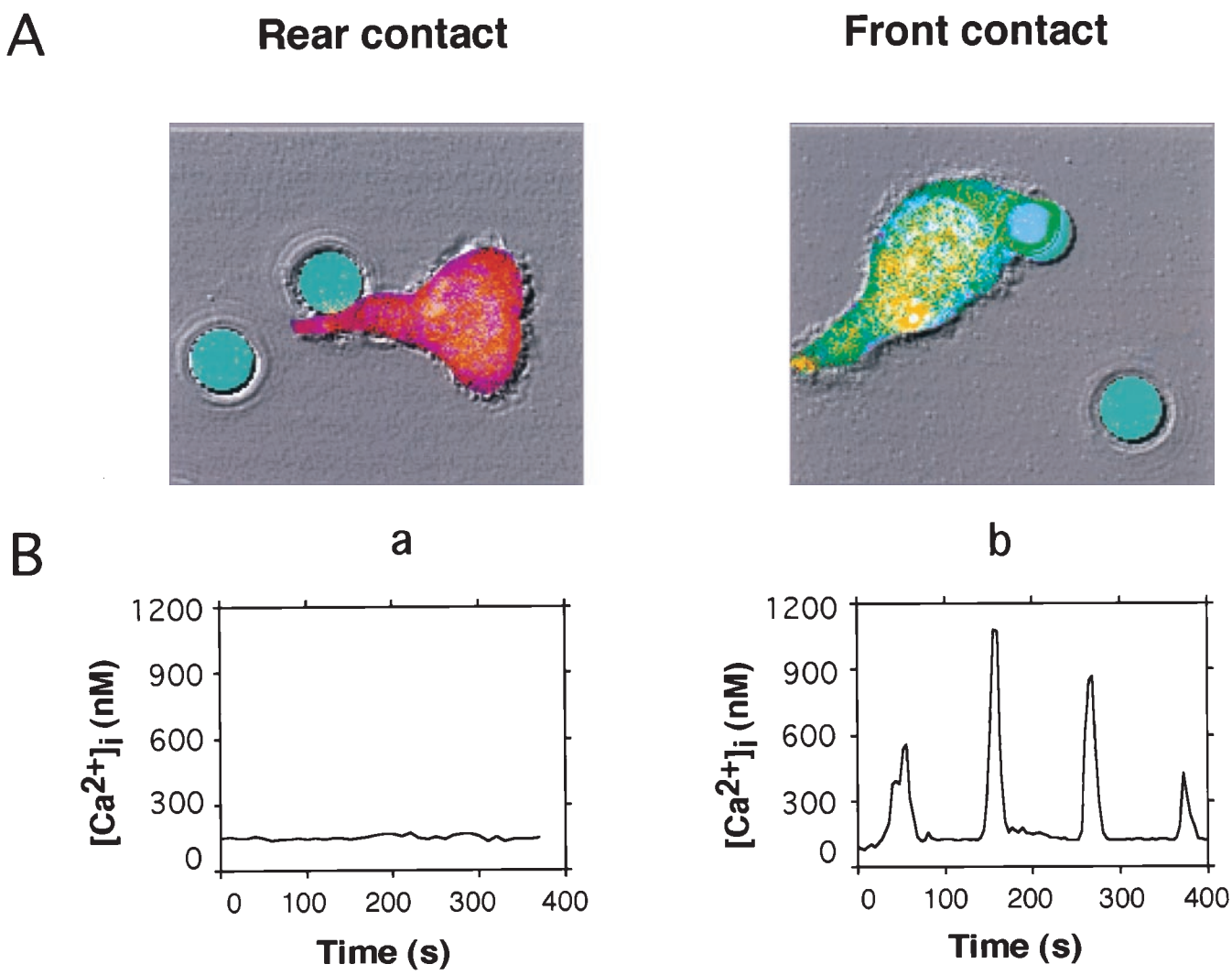


FIG. 1. Optical trapping of anti-CD3 mAb coated-bead identifies functional T cell polarity. (*A*) Bright field and fluorescence images are shown as an overlay. Acetoxymethyl esters of Oregon Green and Fura Red were preincubated with T cells for 90 min. Cells produced a true-color emission shift from red to green when $[Ca^{2+}]_i$ was elevated. Three photomultipliers collected green fluorescence, red fluorescence, and bright field images simultaneously. FITC-conjugated anti-CD3 mAb coated-beads (6.2 $\mu$m in diameter) are shown presented by the optical trap to either the tail (*a*) or leading edge (*b*) of the T cell. (*B*) Time course of $[Ca^{2+}]_i$ for cells shown in *A*. $[Ca^{2+}]_i$ was estimated every 4 s by dividing 488-nm-excited green and red fluorescence images pixel by pixel and applying the equation of Grynkiewicz *et al.* (11).

age of response and the latency of T cell $[Ca^{2+}]_i$ signals depended on anti-CD3 density (Fig. 3). The T cell response percentage steeply increased from 2 to 83%, and the response latency decreased from 160 to 27 s with increasing anti-CD3 mAb density on beads. The half-maximal response corresponded to an anti-CD3 mAb density of 80 per $\mu m^2$. Interestingly, the $[Ca^{2+}]_i$ response pattern switched from transient to oscillating or sustained responses with increasing anti-CD3 mAb density. We arbitrarily chose 18 per $\mu m^2$ as the threshold anti-CD3 mAb density that resulted in 5.3% of T cells displaying $[Ca^{2+}]_i$ response. At this low density, only $[Ca^{2+}]_i$ transients were seen in the responding cells. At higher density ($\geq$60 per $\mu m^2$), sustained or oscillating $[Ca^{2+}]_i$ responses were observed in more than 80% of the trials.

Table 1. Polarized T cell response to TCR stimulation

| Contact zone (on T cell) | Percentage of cell responding (no.) | | | Latency, s | | |
|---|---|---|---|---|---|---|
| | APC | 6.2-$\mu$m bead | 2.5-$\mu$m bead | APC | 6.2-$\mu$m bead | 2.5-$\mu$m bead |
| 1 | 82 (14/17) | 87 (77/87) | 43 (20/46) | 42 ± 16 | 52 ± 23 | 53 ± 16 |
| 2 | 80 (4/5) | 82 (14/17) | — | 60 ± 22 | 141 ± 63 | — |
| 3 | 31 (4/13) | 7 (4/55) | 6 (4/66) | 146 ± 29 | 248 ± 73 | 173 ± 49 |

T cells were stimulated by either APCs or anti-CD3 mAb-coated beads at the region indicated. Region 1 is defined as the leading edge. Latency (mean ± SEM) indicates the delay between contact and a detectable intracellular calcium increase in the responding population.

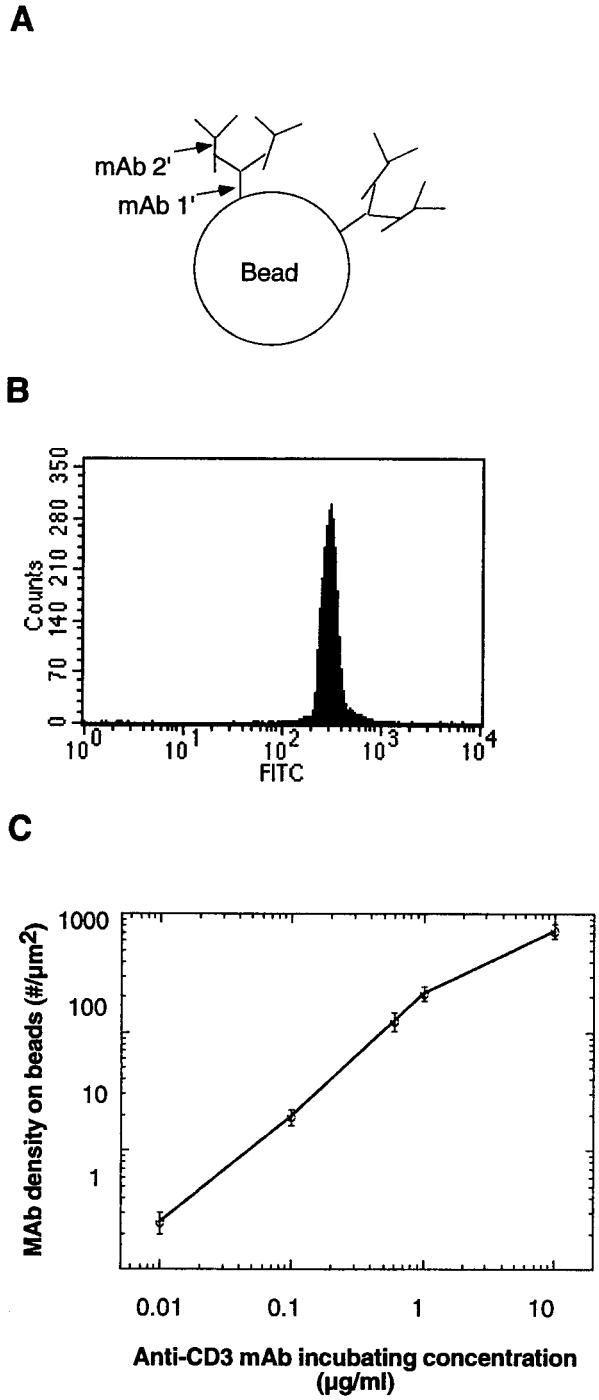


FIG. 2. Quantification of immobilized FITC-conjugated anti-CD3 mAb density on polystyrene beads by FACS analysis. (*A*) Antibody coating on beads. The two-step antibody coating method was assumed to prevent potential steric hindrance and increase anti-CD3 mAb binding efficacy. Beads were initially coated with 100 $\mu$g/ml anti-hamster Fc IgG mAb (mAb 1′) and then with varying concentrations of FITC-conjugated hamster anti-mouse CD3 mAb (mAb 2′) of known fluorescein/protein ratio. mAb 1′ binds the Fc portion of mAb 2′, leaving the antigen-binding site of mAb 2′ free to engage with the TCR:CD3 complex. (*B*) FACS analysis of beads shown in *A*. The number of anti-CD3 mAb on single beads was quantified by using FACS analysis to compare FITC-conjugated mAb-coated beads with a standard curve of microbeads labeled with defined numbers of fluorescein molecules. (*C*) The resulting anti-CD3 mAb density on beads showing a 3-log linearity with incubating antibody concentration.

The flexibility of positioning with the optical tweezers allowed the same contact geometry for each T cell–bead pair so that the contact area between the 5-$\mu$m-diameter bead and the T cell was $\approx$9.5 $\mu m^2$, as determined by a solid-angle measurement. This contact geometry usually did not change until after the $[Ca^{2+}]_i$ rise. Thus, for a bead with anti-CD3 mAb density of 18 per $\mu m^2$, the total number of anti-CD3 mAb molecules on the contact area was $\approx$170. The TCR density on a single T cell is $\approx$300 per $\mu m^2$ (20), corresponding to a spacing of $\approx$0.06 $\mu$m between TCR complexes, and is much higher than the anti-CD3 mAb density on the bead. Because the diffusion constant of the TCR is $\approx$0.01 $\mu m^2/s$ (M. L. Dustin, personal communication; B. Hashemi, D. Holowka, and B. Baird, personal communication), it is not unreasonable to expect that all available antigen-binding sites in the contact region of the low-density beads will become irreversibly occupied by TCRs within the latency period of tens of seconds. Furthermore, assuming the two-step antibody-coating method allows all of the antigen-binding sites of the anti-CD3 mAbs to be available, it is appropriate to estimate the number of triggered TCRs based on the number of anti-CD3 mAb on the contact area. Assuming one bivalent anti-CD3 mAb at most engages 2 TCRs, the number of triggered TCRs at the anti-CD3 mAb threshold density is $\approx$340, corresponding to $\approx$1% of total TCRs on the cell. The actual contact area between the cell and the bead may be smaller than the apparent contact area, considering the local roughness of the T cell surface. Therefore, some portion of the antibody molecules on the estimated contact area may not be able to reach CD3 molecules, despite favorable diffusion. Thus, the number provided here is an upper limit that may underestimate the T cell sensitivity for early signaling.

Analyzing the T cell response latency also provides insight into anti-CD3 mAb threshold density and kinetics for initiating the $[Ca^{2+}]_i$ signal. We assume that the measured latency includes two kinetically distinguishable steps: $T_1$, the time for a fixed number of TCR–mAb complexes to form (21), a function of the stimulating anti-CD3 mAb density; and $T_2$, the minimal time for downstream signal-transduction events leading to the $[Ca^{2+}]_i$ rise. The first step can be approximated as a first-order biochemical reaction with respect to anti-CD3 mAb density, because the density of TCR complexes on a single T cell is higher than the anti-CD3 mAb density. The latency data fit well with this model (Fig. 3*B*, dashed line). The threshold mAb density obtained from the fitting is 13 per $\mu m^2$, which is in agreement with the experimental threshold of 18 per $\mu m^2$ (5.3% T cell response). The constant $T_2$ obtained from the fitting is 23 s, reflecting the minimal time needed for downstream signal transduction events leading to the $[Ca^{2+}]_i$ signal.

Our results suggest that no more than 300–400 TCRs are sufficient to initiate the $[Ca^{2+}]_i$ signal. This number correlates well with previous reports that as few as 100–300 MHC–antigen complexes are sufficient to activate T cells (22–24). However, assuming that a single-hit TCR engagement by its ligand results in internalization of the activated receptor, Viola and Lanzavecchia (3) measured the number of surface TCRs after stimulation and found that T cells count the number of triggered TCRs and respond to produce IFN-$\gamma$ when a threshold of $\approx$8,000 TCRs is reached. Costimulatory signals lowered the activation threshold to $\approx$1,500 TCRs. The $[Ca^{2+}]_i$ rise is an early event in TCR-mediated signaling; later events, including gene expression and cytokine production, may require either more TCRs to be engaged or the presence of costimulation molecules. In addition, different experimental systems, including cell type and experimental methods, might also contribute to the difference. Our results indicate that $\approx$1,000 TCRs are required to generate a long-lasting $[Ca^{2+}]_i$ signal, which might be required for gene expression.

**Minimal Contact Area for Initiating T Cell $[Ca^{2+}]_i$ Response.** To study the contact requirements for T cell $[Ca^{2+}]_i$ response, we varied the size of anti-CD3 mAb-coated beads.

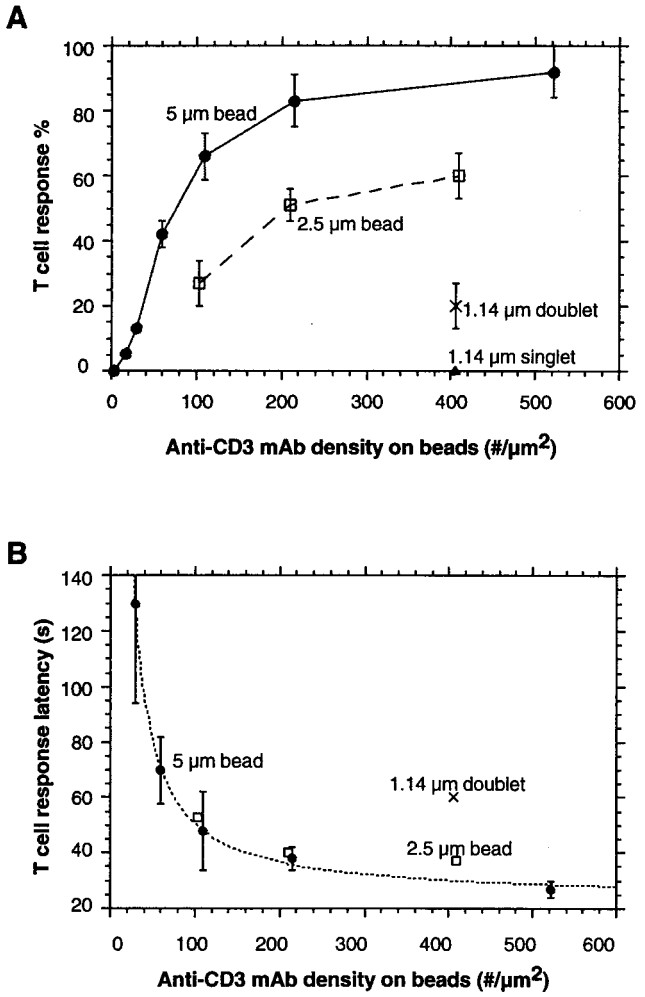


FIG. 3. T cell response depends on anti-CD3 mAb density on beads and contact area between the T cell and the bead ($n$ = 30 cells per point). (*A*) T cell response percentage to beads of varying size and antibody density. Contact areas were 9.5 $\mu m^2$, 4.9 $\mu m^2$, 3.0 $\mu m^2$, and 2.0 $\mu m^2$ for 5-$\mu$m, 2.5-$\mu$m, and 1.14-$\mu$m doublet beads and 1.14-$\mu$m singlet beads, respectively. (*B*) T cell response latencies corresponding to initiation of $[Ca^{2+}]_i$ signals in *A*. Measured response latencies ($T$) for 5-$\mu$m-diameter beads were fit to a pseudo-first-order rate expression with constant offset ($T_2$): $T = K^*\ln[D/(D - A)] + T_2$ (dashed line). $T$, latency time; $D$, anti-CD3 mAb density on beads; $K$, constant; $A$, anti-CD3 mAb threshold density; $T_2$, the minimal time for downstream signal transduction events leading to the $[Ca^{2+}]_i$ rise. The parameters obtained from the fit were $A$ = 13 per $\mu m^2$ and $T_2$ = 23 s. Standard error bars are shown in the figure.

Decreasing the contact area proportionally decreased the T cell $[Ca^{2+}]_i$ response percentage (Fig. 3*A*), suggesting that T cells were able to integrate the stimulus spatially within the range of contact areas. Different sizes of beads with the same amount of mAbs on the contact area achieved similar response percentages. For example, the response percentage for the 2.5-$\mu$m-diameter bead with a mAb density of 103 per $\mu m^2$ was similar to that for the 5-$\mu$m bead with density of 60 per $\mu m^2$. However, a 2.5-$\mu$m-diameter bead with a mAb density of 409 per $\mu m^2$ did not achieve the expected higher response, probably because the antibody density already reached an effective plateau, 150 per $\mu m^2$, corresponding to ≈50% of the TCR density of 300 per $\mu m^2$. The critical contact area seemed to reside at 3 $\mu m^2$, because single 1.14-$\mu$m-diameter beads that contacted T cells with an area of 2 $\mu m^2$ failed to induce the $[Ca^{2+}]_i$ response, even with a very high mAb density of 405 per $\mu m^2$. However, doublets of the same beads with ≈3-$\mu m^2$ contact area achieved an appreciable response percentage (20%; see Fig. 3*A*).

Previously, Mescher (25) reported a 3-$\mu$m-diameter bead-size threshold for effective antigen-dependent degranulation of cytotoxic T lymphocytes when beads coated with alloantigen were added and incubated with a T cell population for 3 h. Ganpule *et al.* (26) found a smaller (1-$\mu$m-diameter) bead-size threshold for integrin-mediated adhesion when a bead-rosetting assay was performed. Although it is difficult to assess the exact contact area in these experiments, the results, together with ours, support the concept that late events in T cell activation, such as cytotoxic T lymphocyte activation and subsequent degranulation, may require a larger surface area. In addition, different stimuli might also contribute to the difference in the contact-area threshold.

The minimal contact area might correspond to a spatial limit for recruiting TCRs and/or other transduction molecule(s). Monks *et al.* (13) recently reported that T cell membrane proteins clustered into segregated three-dimensional domains within the cell-contact zone, and ligand-bound TCR was confined to only 6% of the contact area. The size of this inner contact zone corresponds well with our determination of a minimal contact area of ≈3 $\mu m^2$, suggesting that an inner contact zone of this size may be required to initiate $[Ca^{2+}]_i$ signaling.

## CONCLUSION

We have developed an optical tweezer-based single-cell assay for studying ligand-receptor interactions during T cell activation. This approach allows the geometry and timing of ligand presentation to be controlled precisely so that factors affecting both spatial orientation and activation kinetics can be examined. Our results suggest that no more than 300–400 TCRs are sufficient to initiate the $[Ca^{2+}]_i$ signal, and the minimal contact area is ≈3 $\mu m^2$ (≈0.6% of the total cell plasma surface). This number correlates well with previous reports that as few as 100–300 MHC–antigen complexes are sufficient to activate T cells. The $[Ca^{2+}]_i$ rise is an early event in TCR-mediated signaling, and later events, including gene expression and cytokine production, may require either more TCRs to be engaged or the presence of costimulation molecules. Our results indicate that ≈1,000 TCRs are required to generate a long-lasting $[Ca^{2+}]_i$ signal, which might be required for gene expression. We expect this approach can be combined with ligands for accessory molecules or with downstream assays for gene expression to examine species- and clonal-specific variations in the T cell response and deepen our understanding of the relationship between early activation events and gene expression (27–30).

We thank T. B. Krasieva for excellent technical assistance, P. A. Negulescu and C. Hughes for helpful discussions, and Beckman Laser Institute for programmatic support from the Department of Energy and Office of Naval Research. This work was supported by National Institutes of Health Grants RR01192 (from the Biotechnology Resource Center to B.J.T.) and GM41514 (to M.D.C.).

1. Babbitt, B. P., Allen, P. M., Matsueda, G., Haber, E. & Unanue, E. R. (1985) *Nature (London)* **317,** 359–361.
2. Valitutti, S., Müller, S., Cella, M., Padovan, E. & Lanzavecchia, A. (1995) *Nature (London)* **375,** 148–151.
3. Viola, A. & Lanzavecchia, A. (1996) *Science* **273,** 104–106.
4. Sheetz, M. P. (1998) *Methods Cell Biol.* **55,** 157–171.
5. Yin, H., Wang, M. D., Svoboda, K., Landick, R., Block, S. M. & Gelles, J. (1995) *Science* **270,** 1653–1657.
6. Wang, M. D., Schnitzer, M. J., Yin, H., Landick, R., Gelles, J. & Block, S. M. (1998) *Science* **282,** 902–907.
7. Negulescu, P. A., Krasieva, T. B., Khan, A., Kerschbaum, H. H. & Cahalan, M. D. (1996) *Immunity* **4,** 421–430.

8. Adorini, L., Sette, A., Buus, S., Grey, H. M., Darsley, M., Lehman, P. V., Doria, G., Nagy, Z. A. & Appella, E. (1988) *Proc. Natl. Acad. Sci. USA* **85,** 5181–5185.
9. Berns, M. W., Aist, J. R., Wright, W. H. & Liang, H. (1992) *Exp. Cell Res.* **198,** 375–378.
10. Liang, H., Vu, K. T., Krishnan, P., Trang, T. C., Shin, D., Kimel, S. & Berns, M. W. (1996) *Biophys. J.* **70,** 1529–1533.
11. Grynkiewicz, G., Poenie, M. & Tsien, R. Y. (1985) *J. Biol. Chem.* **260,** 3440–3450.
12. Boniface, J. J. & Davis, M. M. (1995) *Ann. N.Y. Acad. Sci.* **766,** 62–69.
13. Monks, C. R. F., Freiberg, B. A., Kupfer, H., Sciaky, N. & Kupfer, A. (1998) *Nature (London)* **395,** 82–86.
14. Viola, A., Schroeder, S., Sakakibara, Y. & Lanzavecchia, A. (1999) *Science* **283,** 680–682.
15. Kupfer, A. & Singer, S. J. (1989) *Annu. Rev. Immunol.* **7,** 309–337.
16. Wülfing, C. & Davis, M. M. (1998) *Science* **282,** 2266–2269.
17. Kupfer, A., Swain, S. L., Janeway, C. A., Jr., & Singer, S. J. (1986) *Proc. Natl. Acad. Sci. USA* **83,** 6080–6083.
18. Lee, J. K., Black, J. D., Repasky, E. A., Kubo, R. T. & Bankert, R. B. (1988) *Cell* **55,** 807–816.
19. Wülfing, C., Sjaastad, M. D. & Davis, M. M. (1998) *Proc. Natl. Acad. Sci. USA* **95,** 6302–6307.
20. Shaw, A. S. & Dustin, M. L. (1997) *Immunity* **6,** 361–369.
21. Agrawal, N. G. B. & Linderman, J. J. (1995) *Biophys. J.* **69,** 1178–1190.
22. Harding, C. V. & Unanue, E. R. (1990) *Nature (London)* **346,** 574–576.
23. Demotz, S., Grey, H. M. & Sette, A. (1990) *Science* **249,** 1028–1030.
24. Delon, J., Bercovici, N., Raposo, G., Liblau, R. & Trautmann, A. (1998) *J. Exp. Med.* **188,** 1473–1484.
25. Mescher, M. F. (1992) *J. Immunol.* **149,** 2402–2405.
26. Ganpule, G., Knorr, R., Miller, J. M., Carron, C. P. & Dustin, M. L. (1997) *J. Immunol.* **159,** 2685–2692.
27. Sykulev, Y., Brunmark, A., Jackson, M., Cohen, R. J., Peterson, P. A. & Eisen, H. N. (1994) *Immunity* **1,** 15–22.
28. Kageyama, S., Tsomides, T. J., Sykulev, Y. & Eisen, H. N. (1995) *J. Immunol.* **154,** 567–576.
29. Negulescu, P. A., Shastri, N. & Cahalan, M. D. (1994) *Proc. Natl. Acad. Sci. USA* **91,** 2873–2877.
30. Kerschbaum, H. H., Negulescu, P. A. & Cahalan, M. D. (1997) *J. Immunol.* **159,** 1628–1638.